

# Quenched lattice calculation of semileptonic heavy-light meson form factors

G.M. de Divitiis<sup>a,b</sup>, R. Petronzio<sup>a,b</sup>, N. Tantalo<sup>b,c</sup>

<sup>a</sup> *Università di Roma “Tor Vergata”, I-00133 Rome, Italy*

<sup>b</sup> *INFN sezione di Roma “Tor Vergata”, I-00133 Rome, Italy*

<sup>c</sup> *Centro Enrico Fermi, I-00184 Rome, Italy*

We calculate, in the continuum limit of quenched lattice QCD, the matrix elements of the heavy-heavy vector current between heavy-light pseudoscalar meson states. We present the form factors for different values of the initial and final meson masses at finite momentum transfer. In particular, we calculate the non-perturbative correction to the differential decay rate of the process  $B \rightarrow D\ell\nu$  including the case of a non-vanishing lepton mass.

## I. INTRODUCTION

Semileptonic decays of heavy-light mesons play a central role in the study of flavour physics both on the experimental and theoretical sides. The extraction of the Cabibbo–Kobayashi–Maskawa [1, 2] matrix element  $V_{cb}$ , for example, requires the experimental measurement of the decay rate of the process  $B \rightarrow D^{(*)}\ell\nu_\ell$  and the theoretical calculation of the hadron matrix elements of the flavour changing weak currents. A non-perturbative estimate of the matrix elements can be obtained by lattice QCD. Furthermore, within the heavy quark effective theory (HQET) it has been shown [3] that the semileptonic transitions between heavy-light mesons can be parametrized, at leading order of the expansion in the inverse heavy quark mass, in terms of a universal form factor known as Isgur-Wise function. The Isgur-Wise function is universal in the sense that it describes any semileptonic decay mediated by heavy-heavy weak currents regardless of the flavour of the initial and final heavy quarks and of the spins of the mesons. From the phenomenological point of view it is relevant to know the size of the corrections to the Isgur-Wise limit and to establish at which order the heavy quark expansion has to be truncated to produce useful results down to the charm mass.

Matrix elements of the vector heavy-heavy currents between pseudoscalar meson states are parametrized in terms of two form factors. In the case of the light leptons  $\ell = e, \mu$ , the differential decay rate of the process  $B \rightarrow D\ell\nu_\ell$  is proportional to the square of a particular linear combination of the two,  $G^{B \rightarrow D}$ . The BaBar and Belle collaborations have already measured [4, 5] the branching ratios of the processes  $B \rightarrow D^{(*)}\tau\nu_\tau$  and a future measurement of the differential decay rate will make possible to extract  $V_{cb}$  also from this channel. In this case a separate knowledge of the form factors is required, both in the Standard Model and in its minimal extensions (see for example refs. [6, 7]). In ref. [8] we have already shown our final results for  $G^{B \rightarrow D}$  by focusing on their phenomenological implications without giving all the details of the calculation. Here we present detailed results of continuum and chiral extrapolations and separate estimates of the two independent form factors for several values of the initial and final heavy quark masses together with an analysis of the infinite heavy quark mass limit. In addition, we make a prediction for the ratio of the differential decay rates of the processes  $B \rightarrow D\ell\nu_\ell$  with  $\ell = \tau$  and  $\ell = e, \mu$ .

The simulation of relativistic heavy quarks with masses ranging from the physical  $b$  mass down to the physical  $c$  mass has been performed by using the step scaling method (SSM) [9], already applied successfully to the determination of heavy quark masses and heavy-light meson decay constants [10, 11, 12]. The SSM allows to reconcile large quark masses with adequate lattice resolution and large physical volumes. The two form factors have been calculated for different values of the momentum transfer by making use of flavour twisted boundary conditions [13], that shift the discretized set of lattice momenta by an arbitrary amount (see also [14, 15, 16]).

The plan of the paper is as follows. In section II we introduce the form factors in the continuum theory and re-derive the Luke’s theorem [17]. In sections III and IV we set up the lattice notation and describe the calculation. In sections V we discuss the results at finite volumes while in section VI we show our final results. We draw our conclusions in section VII.

## II. FORM FACTORS

The semileptonic decay of a pseudoscalar meson into another pseudoscalar meson is mediated by the vector part of the weak  $V - A$  current. The corresponding matrix element can be parametrized in terms of two form factors,

$$\langle \mathcal{M}_f | V^\mu | \mathcal{M}_i \rangle = (p_i + p_f)^\mu f_+^{i \rightarrow f} + (p_i - p_f)^\mu f_-^{i \rightarrow f}$$

or, equivalently,

$$\frac{\langle \mathcal{M}_f | V^\mu | \mathcal{M}_i \rangle}{\sqrt{M_i M_f}} = (v_i + v_f)^\mu h_+^{i \rightarrow f} + (v_i - v_f)^\mu h_-^{i \rightarrow f} \quad (1)$$

where  $v_{i,f} = p_{i,f}/M_{i,f}$  are the 4-velocities of the mesons. The relations between the  $h_\pm^{i \rightarrow f}$  and the  $f_\pm^{i \rightarrow f}$  parametrizations are given by

$$h_\pm^{i \rightarrow f} = \frac{(M_i + M_f)f_\pm^{i \rightarrow f} + (M_i - M_f)f_\mp^{i \rightarrow f}}{2\sqrt{M_i M_f}}$$

$$f_\pm^{i \rightarrow f} = \frac{(M_i + M_f)h_\pm^{i \rightarrow f} - (M_i - M_f)h_\mp^{i \rightarrow f}}{2\sqrt{M_i M_f}}$$

In the rest of this paper we work in the  $h_\pm^{i \rightarrow f}$  parametrization that, as it will emerge from the discussion below, is more convenient for the study of the dependence of the form factors upon the masses of the initial and final heavy quarks.

The form factors depend upon the masses of the parent and daughter particles and upon  $w \equiv v_f \cdot v_i$

$$h_\pm^{i \rightarrow f}(w) \equiv h_\pm(w, M_i, M_f),$$

Time reversal and hermiticity imply that  $h_+^{i \rightarrow f}$  and  $h_-^{i \rightarrow f}$  are real. Furthermore they imply that  $h_+^{i \rightarrow f}$  is even under the interchange of the initial and final states while  $h_-^{i \rightarrow f}$  is odd,

$$h_+(w, M_i, M_f) = h_+(w, M_f, M_i), \quad h_-(w, M_i, M_f) = -h_-(w, M_f, M_i) \quad (2)$$

In eq. (1) one can consider the limit in which both meson masses go to infinity at fixed 4-velocity; the left hand side is well defined in this limit and, consequently, also the form factors. It is thus legitimate to make a change of variables from the meson masses to the parameters  $\varepsilon_+$  and  $\varepsilon_-$ , defined as

$$\varepsilon_+ = \frac{1}{M_f} + \frac{1}{M_i}, \quad \varepsilon_- = \frac{1}{M_f} - \frac{1}{M_i}$$

Expressed as functions of the new variables,  $h_\pm^{i \rightarrow f} \equiv h_\pm(w, \varepsilon_+, \varepsilon_-)$  are well defined at  $\varepsilon_+ = 0$  and  $\varepsilon_- = 0$  and can be expanded in power series around these points. The symmetry properties of eq. (2) force the odd(even) powers of  $\varepsilon_-$  to vanish into the expansion of  $h_+^{i \rightarrow f}$  ( $h_-^{i \rightarrow f}$ ), i.e.

$$h_+(w, \varepsilon_+, \varepsilon_-) = h_+(w, 0, 0) + \varepsilon_+ \frac{\partial h_+(w, 0, 0)}{\partial \varepsilon_+} + \frac{\varepsilon_+^2}{2} \frac{\partial^2 h_+(w, 0, 0)}{\partial \varepsilon_+^2} + \frac{\varepsilon_-^2}{2} \frac{\partial^2 h_+(w, 0, 0)}{\partial \varepsilon_-^2} + \dots$$

$$h_-(w, \varepsilon_+, \varepsilon_-) = \varepsilon_- \frac{\partial h_-(w, 0, 0)}{\partial \varepsilon_-} + \frac{\varepsilon_- \varepsilon_+}{2} \frac{\partial^2 h_-(w, 0, 0)}{\partial \varepsilon_- \partial \varepsilon_+} + \dots \quad (3)$$

In the elastic case, when the initial and final mesons coincide,  $h_-^{i \rightarrow i}$  vanishes and the vector current is conserved. The conservation of the vector current implies that  $h_+^{i \rightarrow i}(w = 1) = 1$ . This condition, inserted in the previous equations, translates into a condition on the derivatives of  $h_+^{i \rightarrow i}$  with respect to  $\varepsilon_+$

$$\frac{\partial^n h_+(w = 1, 0, 0)}{\partial \varepsilon_+^n} = 0$$

We thus expect that, for values of  $w \simeq 1$  the corrections proportional to  $\varepsilon_+$  will be rather small while the ones proportional to  $\varepsilon_-$ , not constrained by the vector symmetry, can play a role also at zero recoil. This expectation is confirmed by our numerical results (see section VI).

The discussion above is a re-derivation of the "Luke's theorem" [17]. The theorem, originally derived by using HQET arguments, states that  $h_+^{i \rightarrow i}$  it is not affected by first order corrections at zero recoil. In our language

$$h_+(w = 1, \varepsilon_+, \varepsilon_-) = 1 + \frac{\varepsilon_-^2}{2} \frac{\partial^2 h_+(w = 1, 0, 0)}{\partial \varepsilon_-^2} + \dots \quad (4)$$

Eqs. (3) confirm the analysis of the subleading corrections to the form factors that has been carried out by the authors of ref. [18] within HQET<sup>1</sup>. The additional symmetries of the static theory imply relations among the coefficients appearing in eqs. (3) and the corresponding ones arising in the case of vector-pseudoscalar and vector-vector transitions. In particular,  $h_+^{i \rightarrow i}$  is proportional at leading order to the Isgur-Wise function [3].

In ref. [8] we have shown the results concerning the form factor  $G^{B \rightarrow D}(w)$  that enters into the semileptonic decay rate of a  $B$  meson into a  $D$  meson in the approximation of massless leptons  $\ell = e, \mu$ ,

$$\frac{d\Gamma^{B \rightarrow D \ell \nu \ell}}{dw} = |V_{cb}|^2 \frac{G_F^2}{48\pi^3} (M_B + M_D)^2 M_D^3 (w^2 - 1)^{3/2} [G^{B \rightarrow D}(w)]^2$$

$$1 \leq w \leq \frac{M_B^2 + M_D^2}{2M_B M_D}$$

This form factor is related to  $h_+^{i \rightarrow f}(w)$  and  $h_-^{i \rightarrow f}(w)$  by

$$G^{i \rightarrow f}(w) = h_+^{i \rightarrow f}(w) - \frac{M_f - M_i}{M_f + M_i} h_-^{i \rightarrow f}(w)$$

In the case  $\ell = \tau$  the mass of the lepton cannot be neglected and the differential decay rate is given by [6, 19]

$$\frac{d\Gamma^{B \rightarrow D \tau \nu \tau}}{dw} = \frac{d\Gamma^{B \rightarrow D(e, \mu) \nu e, \mu}}{dw} \left(1 - \frac{r_\tau^2}{t(w)}\right)^2 \left\{ \left(1 + \frac{r_\tau^2}{2t(w)}\right) + \frac{3r_\tau^2}{2t(w)} \frac{w+1}{w-1} [\Delta^{B \rightarrow D}(w)]^2 \right\}$$

$$r_\tau = \frac{m_\tau}{M_B}, \quad r = \frac{M_D}{M_B}, \quad t(w) = 1 + r^2 - 2rw,$$

$$1 \leq w \leq \frac{M_B^2 + M_D^2 - m_\tau^2}{2M_B M_D}$$

In this work we provide an estimate of the function  $\Delta^{B \rightarrow D}(w)$  appearing in the previous relations, including values at  $w > 1$ . Its expression in terms of  $h_+^{i \rightarrow f}(w)$  and  $h_-^{i \rightarrow f}(w)$  is given by

$$\begin{aligned} \Delta^{i \rightarrow f}(w) &= \frac{1}{G^{i \rightarrow f}(w)} \left[ \frac{1-r}{1+r} h_+^{i \rightarrow f}(w) - \frac{w-1}{w+1} h_-^{i \rightarrow f}(w) \right] \\ &= \left( \frac{1-r}{1+r} - \frac{w-1}{w+1} \frac{h_-^{i \rightarrow f}(w)}{h_+^{i \rightarrow f}(w)} \right) \left( 1 - \frac{1-r}{1+r} \frac{h_-^{i \rightarrow f}(w)}{h_+^{i \rightarrow f}(w)} \right)^{-1} \end{aligned} \quad (5)$$

---

<sup>1</sup> Some care is needed when eqs. (3) are compared with the corresponding results of ref. [18]. Indeed eqs. (3) are the result of a Taylor expansion and the coefficients do not depend upon  $\varepsilon_{+,-}$  and, consequently, upon the meson masses. Eqs. (B1) of ref. [18] are expansions in inverse powers of the quark masses that depend upon the renormalization scale as well as the coefficients. This dependence cancels at any given order.

In the elastic case  $\Delta^{i \rightarrow f}(w)$  vanishes identically and, in the approximation in which  $h_-^{i \rightarrow f}(w)$  is much smaller than  $h_+^{i \rightarrow f}(w)$ , it is very well approximated by its static limit

$$\Delta^{i \rightarrow f}(w) \simeq \frac{1-r}{1+r}, \quad r = \frac{M_f}{M_i} \quad (6)$$

### III. LATTICE OBSERVABLES

We have carried out the calculation within the  $O(a)$  improved Schrödinger Functional formalism [20, 21] with  $T = 2L$  and vanishing background fields. Physical units have been set by using the Sommer's scale and fixing  $r_0 = 0.5$  fm [22, 23, 24]. In order to set the notations, we introduce the following source operators

$$O_{sr} = \frac{a^6}{L^3} \sum_{\mathbf{y}, \mathbf{z}} \bar{\zeta}_s(\mathbf{y}) \gamma_5 \zeta_r(\mathbf{z}), \quad O'_{sr} = \frac{a^6}{L^3} \sum_{\mathbf{y}, \mathbf{z}} \bar{\zeta}'_s(\mathbf{y}) \gamma_5 \zeta'_r(\mathbf{z})$$

where  $s$  and  $r$  are flavour indexes while  $\zeta$  and  $\zeta'$  are boundary fields at  $x_0 = 0$  and  $x_0 = T$  respectively. The bulk operators are defined according to

$$A_{sr}^0(x) = \bar{\psi}_s(x) \gamma_5 \gamma^0 \psi_r(x), \quad P_{sr}(x) = \bar{\psi}_s(x) \gamma_5 \psi_r(x) \quad \mathcal{A}_{sr}^0(x) = A_{sr}^0(x) + ac_A \frac{\partial_0 + \partial_0^*}{2} P_{sr}(x)$$

$$V_{sr}^\mu(x) = \bar{\psi}_s(x) \gamma^\mu \psi_r(x), \quad T_{sr}^{\mu\nu}(x) = \bar{\psi}_s(x) \gamma^\mu \gamma^\nu \psi_r(x) \quad \mathcal{V}_{sr}^\mu(x) = V_{sr}^\mu(x) + ac_V \frac{\partial_\nu + \partial_\nu^*}{2} T_{sr}^{\mu\nu}(x)$$

The improvement coefficient  $c_A$  has been computed non-perturbatively in ref. [25]. Regarding  $c_V$ , we have used the perturbative result from ref. [26] but its actual value influences our results at the level of a few per mille.

The quark masses have been defined through the PCAC relation. We have calculated the following correlation functions

$$f_{sr}^A(x_0) = - \sum_{\mathbf{x}} \langle O_{rs} A_{sr}^0(x) \rangle \quad f_{sr}^P(x_0) = - \sum_{\mathbf{x}} \langle O_{rs} P_{sr}(x) \rangle$$

and defined

$$m_r^{AWI} = \frac{1}{2f_{rr}^P} \left[ \frac{\partial_0 + \partial_0^*}{2} f_{rr}^A + ac_A \partial_0 \partial_0^* f_{rr}^P \right], \quad am_r^{VWI} = \frac{1}{2} \left[ \frac{1}{k_r} - \frac{1}{k_c} \right]$$

where  $a$  is the lattice spacing,  $k_r$  is the hopping parameter of the  $r$  quark and  $k_c$  is the critical value of the hopping parameter. The renormalization group invariant (RGI) quark masses have been obtained by the following relation

$$m_r = Z_M [1 + (b_A - b_P) am_r^{VWI}] m_r^{AWI} \quad (7)$$

The combination  $b_A - b_P$  of the improvement coefficients of the axial current and pseudoscalar density has been computed non-perturbatively in [27, 29]. The factor  $Z_M$  is known with very high precision in a range of inverse bare couplings that does not cover all the values of  $\beta$  used in our simulations. We have used the results reported in table 6 of ref. [28] to parametrize  $Z_M$  in the enlarged range of  $\beta$  values [5.9, 7.6].

In order to define on the lattice the matrix elements of the vector current between pseudoscalar meson states, we need to introduce other two correlation functions,

$$\mathcal{F}_{i \rightarrow f}^\mu(x_0; \mathbf{p}_i, \mathbf{p}_f) = \frac{a^3}{2} \sum_{\mathbf{x}} \langle O_{li} \mathcal{V}_{if}^\mu(x) O'_{fl} \rangle, \quad f_{\mathcal{A}}^f(x_0, \mathbf{p}_f) = - \sum_{\mathbf{x}} \langle O_{lf} \mathcal{A}_{fl}^0(x) \rangle$$

where  $i$  and  $f$  are the heavy flavour indexes and  $l$  is the light one. The external momenta have been set by using flavour twisted b.c. for the heavy flavours; in particular we have used

$$\psi_{i,f}(x + \hat{1}L) = e^{i\theta_{i,f}} \psi_{i,f}(x), \quad p_1 = \frac{\theta_{i,f}}{L} + \frac{2\pi k_1}{L}, \quad k_1 \in \mathbb{N}$$

and ordinary periodic b.c. in the other spatial directions and for the light quarks. We have worked in the Lorentz frame in which the parent particle is at rest ( $\mathbf{p}_i = \mathbf{0}$ ). In this frame  $w$  is simply expressed in terms of the ratio between the energy and the mass of the daughter particle  $w = E_f/M_f$ . The matrix elements of  $V^\mu$  have been defined by the following ratios

$$\langle V^\mu \rangle_{D1}^{i \rightarrow f} \equiv \langle \mathcal{M}_f | V^\mu | \mathcal{M}_i \rangle_{D1} \equiv 2\sqrt{M_i E_f} \frac{\mathcal{F}_{i \rightarrow f}^\mu(T/2; \mathbf{0}, \mathbf{p}_f)}{\sqrt{\mathcal{F}_{i \rightarrow i}^0(T/2; \mathbf{0}, \mathbf{0}) \mathcal{F}_{f \rightarrow f}^0(T/2; \mathbf{p}_f, \mathbf{p}_f)}} \quad (8)$$

that become the physical matrix elements in large volumes where single state dominance is a good approximation. An alternative definition of the matrix elements ( $D2$ ), which reduces to the previous one ( $D1$ ) in the infinite volume and at zero lattice spacing, can be obtained by considering

$$\langle V^\mu \rangle_{D2}^{i \rightarrow f} \equiv \langle \mathcal{M}_f | V^\mu | \mathcal{M}_i \rangle_{D2} \equiv 2 \frac{\sqrt{M_i} E_f f_A^f(T/2, \mathbf{0})}{\sqrt{M_f} f_A^f(T/2, \mathbf{p}_f)} \frac{\mathcal{F}_{i \rightarrow f}^\mu(T/2; \mathbf{0}, \mathbf{p}_f)}{\sqrt{\mathcal{F}_{i \rightarrow i}^0(T/2; \mathbf{0}, \mathbf{0}) \mathcal{F}_{f \rightarrow f}^0(T/2; \mathbf{0}, \mathbf{0})}} \quad (9)$$

In eqs. (8) and (9) the renormalization factors  $Z_V$  and  $Z_A$  cancel in the ratios together with the factors containing the improvement coefficients  $b_V$  and  $b_A$ .

By calculating the following ratio

$$x_f = \frac{\mathcal{F}_{f \rightarrow f}^1(T/2; \mathbf{0}, \mathbf{p}_f)}{\mathcal{F}_{f \rightarrow f}^0(T/2; \mathbf{0}, \mathbf{p}_f)} = \frac{\langle \mathcal{M}_f | \mathcal{V}^1 | \mathcal{M}_f \rangle}{\langle \mathcal{M}_f | \mathcal{V}^0 | \mathcal{M}_f \rangle} = \frac{\sqrt{w^2 - 1}}{w + 1}$$

we have defined  $w$ , as well as meson masses and energies, entirely in terms of three point correlation functions. This definition of  $w$  is noisier than the one that can be obtained in terms of ratios of two point correlation functions; however it leads to exact vector current conservation when  $M_f = M_i$  and reduces the final statistical error on the form factors. The two definitions of the matrix elements lead to two definitions of the form factors that, in terms of  $\langle V^0 \rangle_D$  and  $\langle V^1 \rangle_D$ , are expressed by

$$h_+^{i \rightarrow f}(w) = \frac{\langle V^0 \rangle^{i \rightarrow f}}{2M_i \sqrt{r}} \left\{ 1 + \frac{\sqrt{w^2 - 1}}{w + 1} \frac{\langle V^1 \rangle^{i \rightarrow f}}{\langle V^0 \rangle^{i \rightarrow f}} \right\} \quad (10)$$

$$h_-^{i \rightarrow f}(w) = \frac{\langle V^0 \rangle^{i \rightarrow f}}{2M_i \sqrt{r}} \left\{ 1 + \frac{w + 1}{\sqrt{w^2 - 1}} \frac{\langle V^1 \rangle^{i \rightarrow f}}{\langle V^0 \rangle^{i \rightarrow f}} \right\} \quad (11)$$

$$G^{i \rightarrow f}(w) = \frac{2r}{1 + r} \frac{\langle V^0 \rangle^{i \rightarrow f}}{2M_i \sqrt{r}} \left\{ 1 + \frac{wr - 1}{r\sqrt{w^2 - 1}} \frac{\langle V^1 \rangle^{i \rightarrow f}}{\langle V^0 \rangle^{i \rightarrow f}} \right\}, \quad r = \frac{M_f}{M_i} \quad (12)$$

The last two equations are not defined at  $w = 1$ ; this is due to the second term in the parenthesis of eq. (11) and (12) that we extrapolate at zero recoil before calculating  $h_-^{i \rightarrow f}(w = 1)$  and  $G^{i \rightarrow f}(w = 1)$ .

#### IV. THE STEP SCALING METHOD

The SSM has been introduced to cope with two-scale problems in lattice QCD. In the calculation of heavy-light meson properties the two scales are the mass of the heavy quarks ( $b, c$ ) and the mass of the light quarks ( $u, d, s$ ). Here we consider the generic form factor  $F^{i \rightarrow f} = \{h_+^{i \rightarrow f}, h_-^{i \rightarrow f}, G^{i \rightarrow f}\}$  as a function of  $w$ , the volume  $L^3$  and fix the meson states by the corresponding heavy and light RGI quark masses that, being extracted by the lattice version of the PCAC relation, are not affected by finite volume effects (see eq. 7).

The first step of the finite volume recursion consists in calculating the observable  $F^{i \rightarrow f}(w; L_0)$  on a small volume,  $L_0$ , which is chosen to accommodate the dynamics of heavy quarks with masses ranging from the physical value of the charm mass up to the mass of the bottom. As in our previous work we fixed  $L_0 = 0.4$  fm. We have simulated five different heavy quark masses  $m_{i,f} = \{m_h^1, m_h^2, m_h^3, m_h^4, m_h^5\}$ , five different momenta  $\theta_1 = \{\theta_1^1, \theta_1^2, \theta_1^3, \theta_1^4, \theta_1^5\}$  (see eq. (8)) and three light quark masses  $m_l = \{m_l^1, m_l^2, m_l^3\}$ .

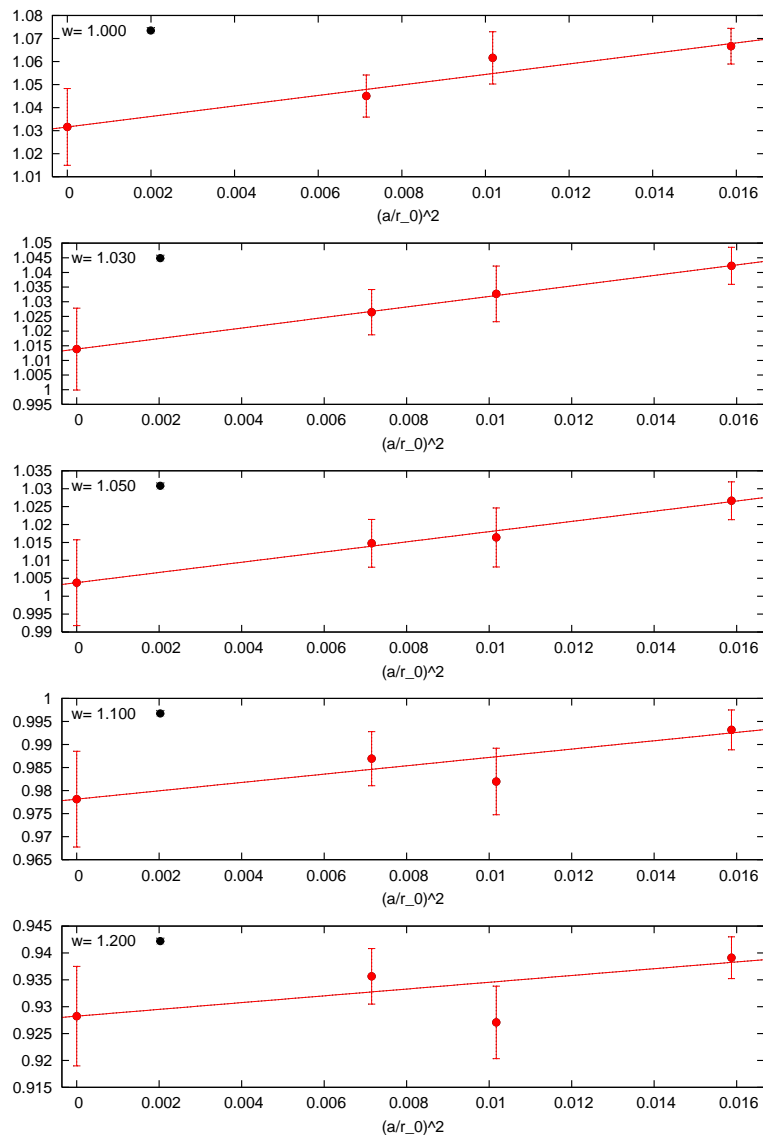


FIG. 1: Extrapolations to the continuum limit of  $G^{B \rightarrow D}(w)$ . The data correspond to  $m_l = m_s$ , to the definition  $D1$  and to the data sets  $L_0A$ ,  $L_0B$  and  $L_0C$ .

A first effect of finite volume is taken into account by evolving the results from  $L_0$  to  $L_1 = 0.8$  fm through the factor

$$\sigma^{i \rightarrow f}(w; L_0, L_1) = \frac{F^{i \rightarrow f}(w; L_1)}{F^{i \rightarrow f}(w; L_0)}$$

computed for each value of  $w$  and for each value of the light quark mass. The crucial point is that the step scaling functions are calculated by simulating heavy quark masses smaller than the  $b$ -quark mass. The step scaling functions at  $m_i \simeq m_b$  and  $m_f \simeq m_c$  are obtained by directly simulating  $m_f$  both on  $L_0$  and on  $L_1$  and by a smooth extrapolation in  $1/m_i$ .

Extrapolating the step scaling functions is more advantageous than extrapolating the form factors. This can be easily

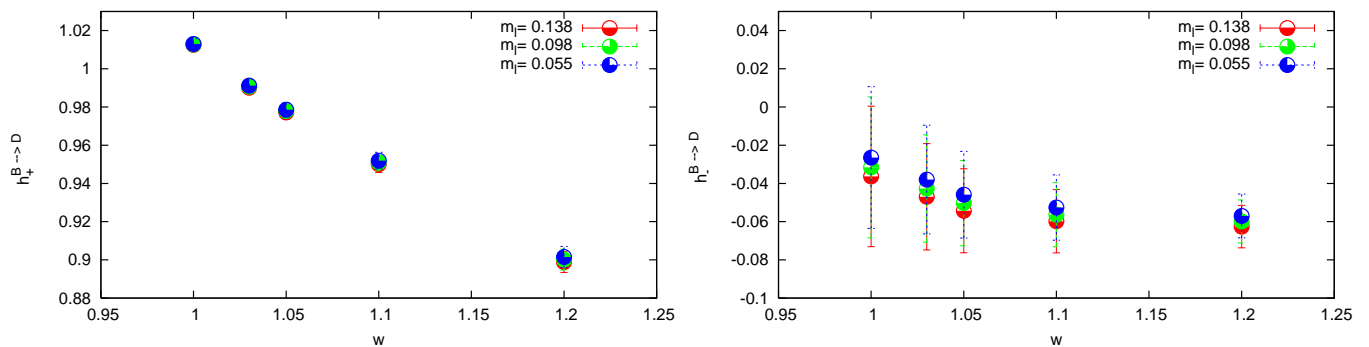


FIG. 2: Light quark mass dependence of  $h_+^{B \rightarrow D}(w; L_0)$  (left) and of  $h_-^{B \rightarrow D}(w; L_0)$  (right). The different sets of points correspond to different values of  $m_l$  ranging from about  $m_s$  to about  $m_s/4$ . The data are in the continuum limit and correspond to the definition D1.

understood by relying on HQET expectations (see also eq. (3)),

$$\begin{aligned}
 \sigma^{i \rightarrow f}(w; L_0, L_1) &= \frac{F^{(0) \rightarrow f}(w; L_1) \left[ 1 + \frac{F^{(1) \rightarrow f}(w; L_1)}{m_i} + \dots \right]}{F^{(0) \rightarrow f}(w; L_0) \left[ 1 + \frac{F^{(1) \rightarrow f}(w; L_0)}{m_i} + \dots \right]} \\
 &= \frac{F^{(0) \rightarrow f}(w; L_1)}{F^{(0) \rightarrow f}(w; L_0)} \left[ 1 + \frac{F^{(1) \rightarrow f}(w; L_1) - F^{(1) \rightarrow f}(w; L_0)}{m_i} + \dots \right] \\
 &\equiv \sigma^{(0) \rightarrow f}(w; L_0, L_1) \left[ 1 + \frac{\sigma^{(1) \rightarrow f}(w; L_0, L_1)}{m_i} + \dots \right]
 \end{aligned}$$

In the previous relations the superscripts in parenthesis, ( $n$ ), mark the order of the expansion in the inverse heavy quark mass. The subleading correction to the step scaling functions is the difference of two terms and vanishes in the infinite volume,  $\sigma^{(1) \rightarrow f}(w; L_0, L_1) = F^{(1) \rightarrow f}(w; L_1) - F^{(1) \rightarrow f}(w; L_0)$ , becoming smaller and smaller as the volume is increased. This matches the general idea that finite volume effects, measured by the  $\sigma$ 's, are almost insensitive to the high energy scale.

We also compute the step scaling functions of the elastic form factors  $h_+^{i \rightarrow i}$  at  $m_i \simeq m_b$  by extrapolating the corresponding results from smaller heavy quark masses. Also in this case the  $\sigma$ 's are expected to be almost flat with respect to  $1/m_i$ .

In order to remove the residual finite volume effects we iterate the procedure described above once more passing from  $L_1$  to  $L_2 = 1.2$  fm. Our final results are obtained from

$$F^{i \rightarrow f}(w; L_2) = F^{i \rightarrow f}(w; L_0) \sigma^{i \rightarrow f}(w; L_0, L_1) \sigma^{i \rightarrow f}(w; L_1, L_2) \quad (13)$$

## V. FINITE VOLUME RESULTS

### A. small volume

The small volume  $L_0 = 0.4$  fm has been simulated by using three different values of the lattice spacing (see table II). The small physical extent of the volume allowed us to simulate relativistic heavy quarks with masses ranging from around  $m_b$  down to  $m_c$ . We have computed the form factors  $h_+^{i \rightarrow f}$ ,  $h_-^{i \rightarrow f}$  and  $G^{i \rightarrow f}$  for all the combinations of heavy and light quark masses and for five different values of the momentum transfer.

In figure 1 we show the continuum extrapolations of  $G^{B \rightarrow D}(w)$ . The points in this figure correspond to  $m_l = m_s$  but similar figures can be obtained for the other values of the light and heavy quark masses and for the other form factors.

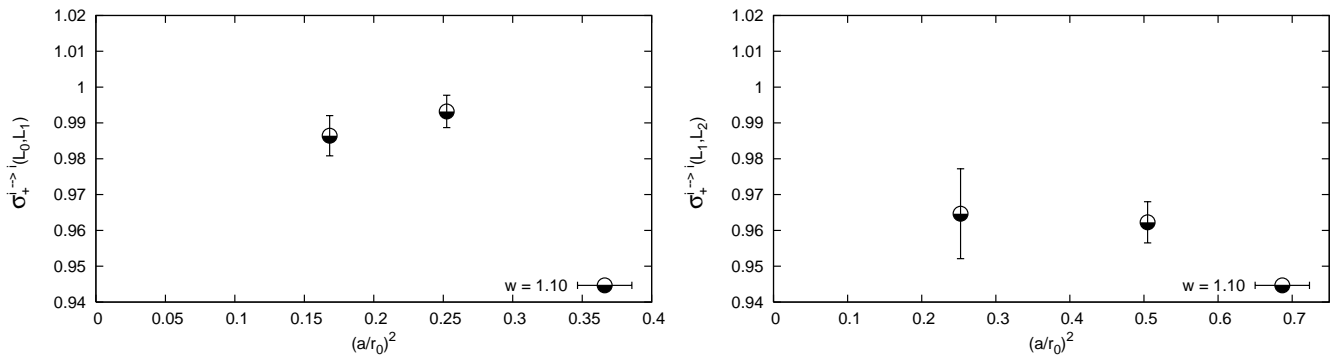


FIG. 3: Continuum extrapolation of  $\sigma_{+^{i \rightarrow i}}^{i \rightarrow i}(w = 1.1; L_0, L_1)$  (left) and  $\sigma_{+^{i \rightarrow i}}^{i \rightarrow i}(w = 1.1; L_1, L_2)$  (right) at the heaviest values of the heavy quark masses ( $m_i \simeq m_b/4$  and  $m_i \simeq m_b/2$  respectively). The data correspond to  $m_l = m_s$ , to the definition *D1* and to the data sets  $L_1A/L_0a$ ,  $L_1B/L_0b$  (left) and  $L_2A/L_1a$ ,  $L_2B/L_1b$  (right).

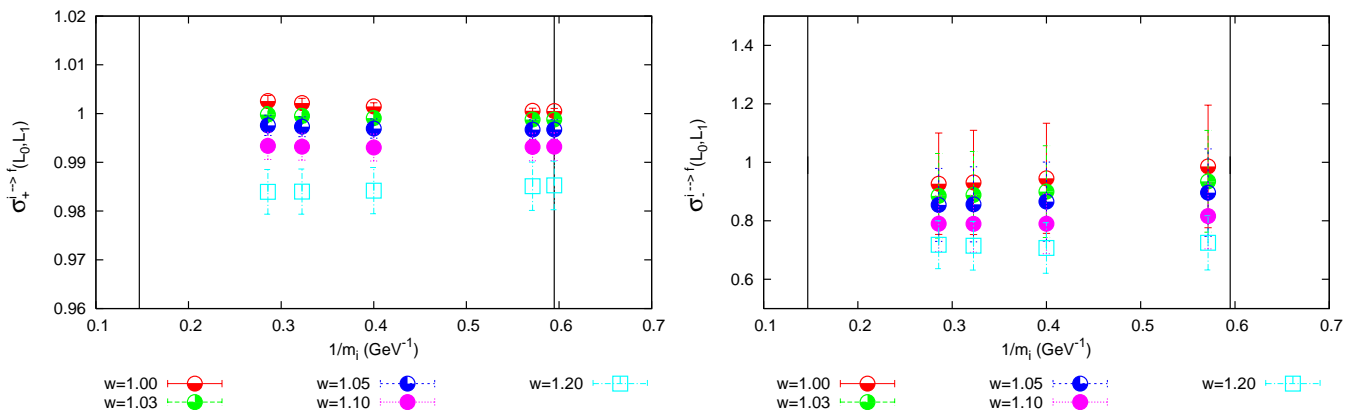


FIG. 4: Step scaling functions of  $h_{+}^{B \rightarrow c}$  (left) and  $h_{-}^{B \rightarrow c}$  (right) as functions of  $1/m_i$  for the first evolution step (from  $L_0$  to  $L_1$ ). The black vertical lines represent the physical points  $m_i = m_c$  and  $m_i = m_b$ . The data are in the continuum and chiral limits and correspond to the definition *D1*.

In figure 2 we show  $h_{+}^{B \rightarrow D}$  (left) and  $h_{-}^{B \rightarrow D}$  (right) as functions of  $w$  for the three different values of light quark masses that we have simulated (ranging from about  $m_s$  to  $m_s/4$ ). As we have anticipated in ref. [8], we find that the  $F$ 's behave as constants with respect to  $m_l$  within the statistical errors. This happens for each combination of heavy quark masses and for each value of the lattice spacing. Nevertheless we make a linear extrapolation to reach the chiral limit; the resulting error largely accounts for the systematics due to these extrapolations. In the following our results include the mild chiral extrapolation.

## B. steps

The parameters of the simulations of the evolution steps are given in tables IV and VI. We have been simulating at two different lattice spacings by limiting the maximum value of the heavy quark mass to  $m_i \simeq m_b/2$  for the first step and to  $m_i \simeq m_b/4$  for the second. In figure 3 we show the dependence upon the lattice spacing of the step scaling functions  $\sigma_{+^{i \rightarrow f}}^{i \rightarrow f}(w = 1.1; L_0, L_1)$  (left) and  $\sigma_{+^{i \rightarrow f}}^{i \rightarrow f}(w = 1.1; L_1, L_2)$  (right) in the worst case (largest value of heavy quark masses). In general our results are consistent with a scaling regime within a few per mille accuracy and the continuum step scaling functions of tables V and VII have been obtained by averaging the results at the two lattice spacings.

In figure 4 we can test our hypothesis on the low sensitivity of the step scaling functions upon the high energy scale. The figure shows the step scaling functions of the form factors  $h_{+}^{i \rightarrow c}$  (left) and  $h_{-}^{i \rightarrow c}$  (right) as functions of  $1/m_i$ . In both cases the dependence upon  $m_i$  is hardly appreciable and in the case of  $h_{+}^{i \rightarrow c}$  the  $\sigma$ 's are very close to one while  $h_{-}^{i \rightarrow c}$  is affected by stronger finite volume effects. We obtain the values at  $m_i = m_b$  by linear fits.



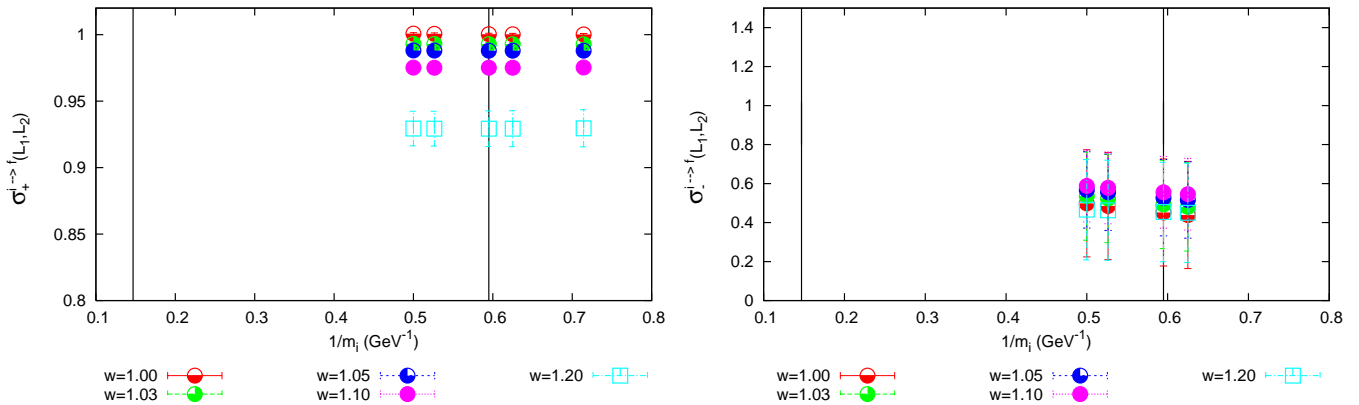


FIG. 5: Step scaling functions of  $h_+^{i \rightarrow f}$  (left) and  $h_-^{i \rightarrow f}$  (right) at fixed  $m_f$  as functions of  $1/m_i$  for the second evolution step (from  $L_1$  to  $L_2$ ). The black vertical lines represent the physical points  $m_i = m_c$  and  $m_i = m_b$ . The data are in the continuum and chiral limits and correspond to the definition  $D1$ .

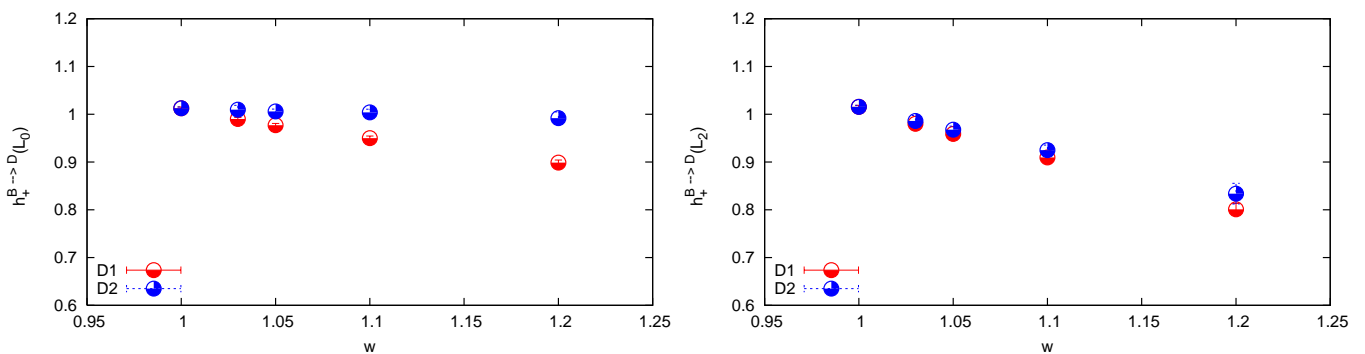


FIG. 6: Comparison of the two definitions of  $h_+^{B \rightarrow D}(w; L)$  at  $L_0 = 0.4$  fm (left) and at  $L_2 = 1.2$  fm (right). The data are in the continuum and chiral limits.

In figure 5 we plot the same quantities as in figure 4 for the second evolution step (from  $L_1$  to  $L_2$ , see table VI). Also in this case the step scaling functions depend very smoothly upon  $1/m_i$ .

### C. consistency checks

In this section we illustrate the results of two checks that we have done in order to convince ourselves on the consistency of the step scaling procedure. As already discussed in sec. III, we have used two different definitions of the matrix elements and, consequently, of each form factor. In figure 6 we show the comparison of  $h_+^{B \rightarrow D}(w; L)$  at  $L_0 = 0.4$  fm (left) and at  $L_2 = 1.2$  fm (right). We see that the results, while differing at finite volume, converge to common values after the step scaling procedure. This makes us confident of a correct accounting of finite volume effects.

A second check of the whole procedure, and in particular of the continuum limit of the step scaling functions, can be obtained by considering the elastic form factor  $h_+^{D \rightarrow D}(w; L)$  at fixed  $w$  as a function of  $L$ . The point is that the charm quark mass has been simulated directly on each physical volume and, in particular, on the biggest one. In figure 7 we fix  $w = 1.05$  (left) and  $w = 1.10$  (right) and see that the step scaling recursion (black points) converge to the result obtained directly at  $L_2 = 1.2$  fm (red points, slightly displaced to help the eye) making us confident of a correct accounting of the cutoff effects and, in particular, of a correct estimate of the error on the continuum step scaling functions.

Our final results are obtained by averaging over the two definitions and by combining in quadrature statistical errors with the systematic ones that we estimate from the dispersion between  $D1$  and  $D2$ .

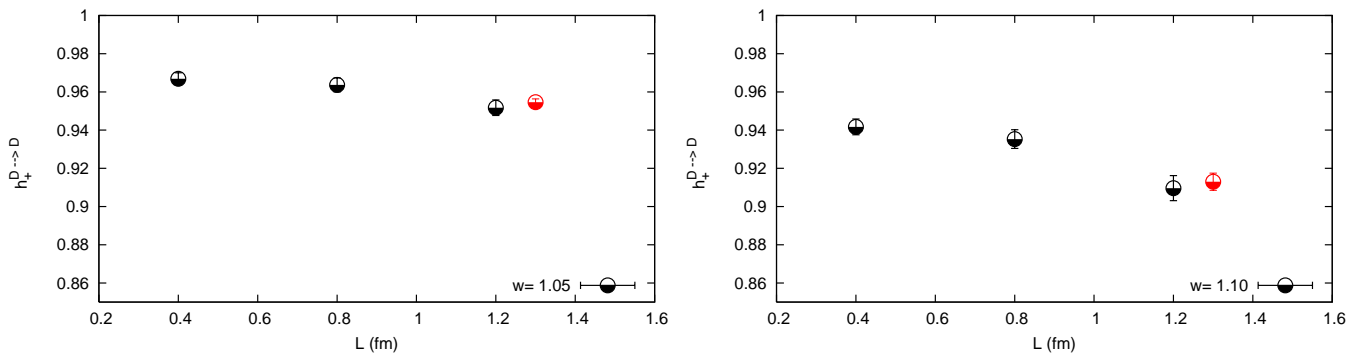


FIG. 7:  $h_+^{D \rightarrow D}(w = 1.05; L)$  (left) and  $h_+^{D \rightarrow D}(w = 1.10; L)$  (right) as functions of the volume. The black points have been obtained through the step scaling recursion while the red points (slightly displaced on the  $x$ -axis to help the eye) are the result of a direct simulation on the biggest volume. The data are in the continuum and chiral limits and correspond to the definition D1.

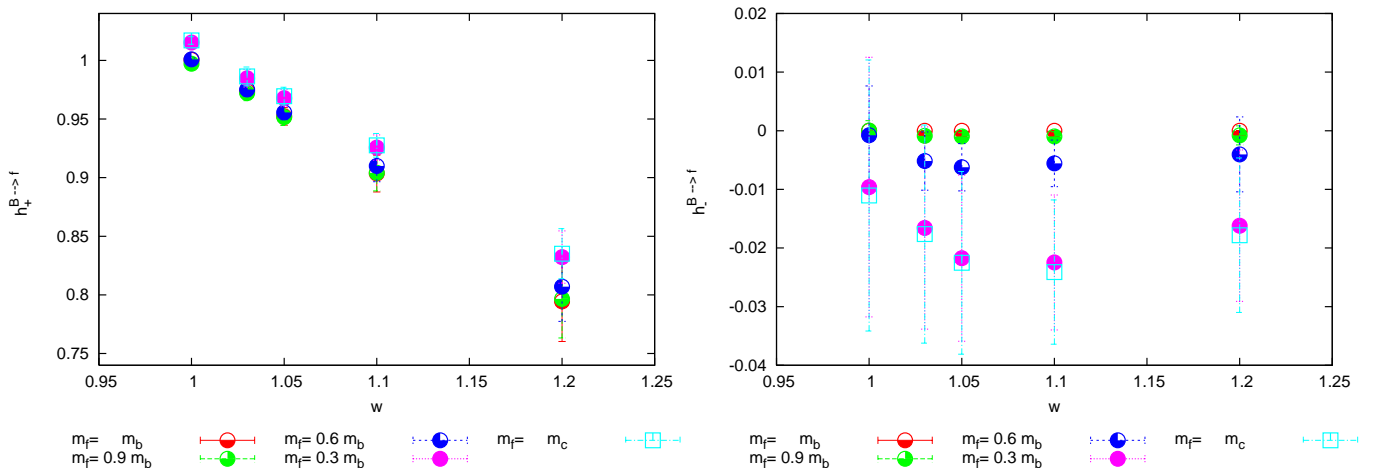


FIG. 8: In the left plot it is shown  $h_+^{B \rightarrow f}(w)$  in the infinite volume limit as a function of  $w$  for different values of the final heavy quark mass. The right plot shows  $h_-^{B \rightarrow f}(w)$  for the same combinations of heavy quark masses.

## VI. FINAL RESULTS

In this section we discuss our final results in the continuum, chiral and infinite volume limits (table I). In order to establish the onset of the static limit approximation we plot in figure 8 the form factor  $h_+^{B \rightarrow f}(w)$  as a function of  $w$  for different values of the final heavy quark mass. The right plot shows  $h_-^{B \rightarrow f}(w)$  for the same combinations of heavy quark masses. We see that the corrections to the static limits of both  $h_+^{B \rightarrow f}(w)$  and  $h_-^{B \rightarrow f}(w)$  are of the order of 2% at the charm mass. For heavy quark masses bigger than  $m_b/2$  the corrections are almost negligible (below 1%).

Eqs. (3) and (4) predict that the convergence toward the static limit is faster in the case of the elastic form factors with respect to the ones having  $m_i > m_f$ . This happens because near the point at zero recoil the subleading corrections to  $h_+^{i \rightarrow f}(w)$  are proportional to the square of the difference of the initial and final meson masses. Figure 9 clearly shows that this happens in practice. Indeed, in the left plot we see that the elastic form factor  $h_+^{D \rightarrow D}(w)$  is much closer to the static limit (very well approximated by  $h_+^{B \rightarrow B}(w)$ ) with respect to the form factor  $h_+^{B \rightarrow D}(w)$ , the one relevant into the calculation of  $V_{cb}$  shown in figure 8. In the right plot of figure 9 we show how well eq. (4) is approximated by our numerical data. The fit is performed on the slope while the intercept is fixed to one.

The QCD form factor  $h_+^{i \rightarrow f}(w)$  is related to the renormalization group invariant HQET Isgur-Wise function,  $\xi(w)$ , by the following relation [30, 31]

$$h_+^{i \rightarrow f}(w) = \left[ 1 + \beta_+(m_i, m_f; w) + \gamma_+(m_i, m_f; w) + O(m_{i,f}^{-2}) \right] \xi(w)$$

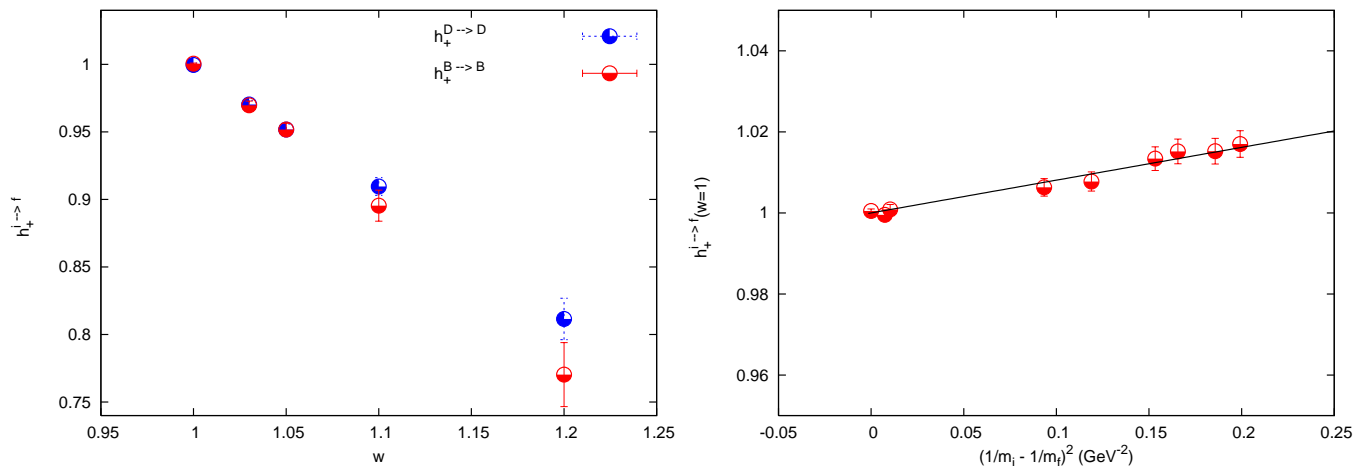


FIG. 9: The left plot shows  $h_+^{B \to B}(w)$  and  $h_+^{D \to D}(w)$ : in the range  $1 \leq w \leq 1.05$  the two elastic form factors are indistinguishable within the quoted errors while  $h_+^{B \to D}(w)$  in fig. 8 shows appreciable corrections from the Isgur-Wise limit, in particular at zero recoil. The right plot shows  $h_+^{i \to f}$  at zero recoil ( $w = 1$ ) as a function of  $\varepsilon_-^2$  (actually  $(1/m_i - 1/m_f)^2 \propto \varepsilon_-^2$ ,  $m_{i,f}$  being the RGI heavy quark masses): the solid line has been obtained by fitting the data according to eq. (4).

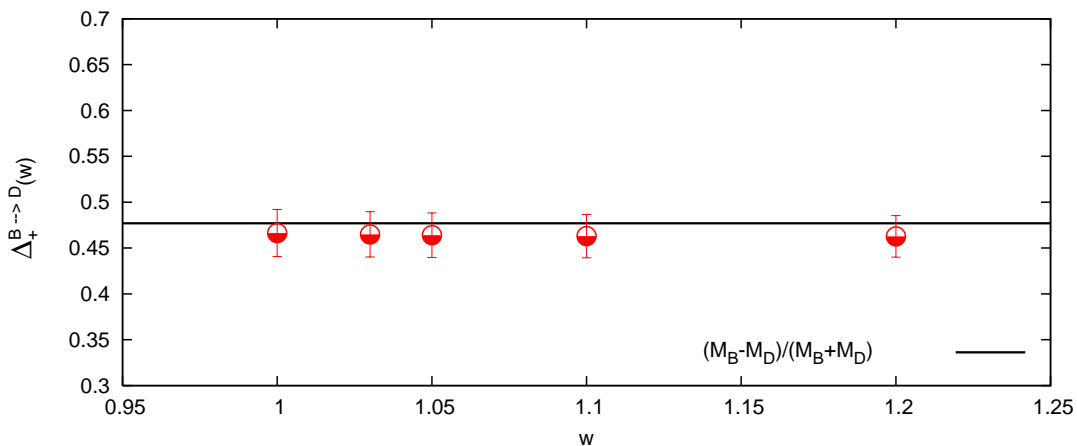


FIG. 10: The figure shows the function  $\Delta_+^{B \to D}(w)$  in the chiral, continuum, and infinite volume limits. The solid line correspond to the static limit result,  $(M_B - M_D)/(M_B + M_D)$ , and has been drawn by using the experimental determinations of the meson masses.

where the  $\gamma_+$  term accounts for non-perturbative power corrections proportional to the inverse of the quark masses while the  $\beta_+$  term accounts for perturbative radiative corrections. In the case of the elastic form factor  $h_+^{i \to i}(w)$  at the highest value of the simulated heavy quark masses, i.e. the bottom quark mass, power corrections are completely negligible in our data as clearly emerges from figures 8 and 9:

$$\gamma_+(m_b, m_b; w) \cong 0$$

$$h_+^{B \to B}(w) = [1 + \beta_+(m_b, m_b; w)] \xi(w)$$

The function  $\beta_+(m_b, m_b; w)$  depends logarithmically upon the bottom mass through  $\alpha_s(m_b)$  and vanishes at zero recoil where the renormalized Isgur-Wise function is identically equal to one like the relativistic QCD elastic form factor. These terms are of the percent order and their logarithmic dependence upon  $m_b$  cannot be extrapolated away from our data. Nevertheless, in order to get the HQET Isgur-Wise function our non-perturbative results for  $h_+^{B \to B}(w)$  (given in table I) can be further corrected by hand through the perturbative  $\beta_+(m_b, m_b; w)$  given in ref. [30] at next

$i \rightarrow f$	$w$	$G$	$h_+$	$h_-$	$\Delta$
$D \rightarrow D$	1.00	1.000(00)	1.000(00)		
	1.03	0.971(07)	0.971(07)		
	1.05	0.955(06)	0.955(06)		
	1.10	0.916(09)	0.916(09)		
	1.20	0.828(20)	0.828(20)		
$B \rightarrow B$	1.00	1.000(00)	1.000(00)		
	1.03	0.974(07)	0.974(07)		
	1.05	0.952(07)	0.952(07)		
	1.10	0.903(16)	0.903(16)		
	1.20	0.794(34)	0.794(34)		
$B \rightarrow D$	1.00	1.026(17)	1.017(03)	-0.011(23)	0.466(26)
	1.03	1.001(19)	0.986(08)	-0.018(19)	0.465(25)
	1.05	0.987(15)	0.970(07)	-0.023(16)	0.464(24)
	1.10	0.943(11)	0.928(10)	-0.024(12)	0.463(24)
	1.20	0.853(21)	0.835(21)	-0.018(13)	0.463(23)

TABLE I: Physical results. Average of the two definitions  $D1$  and  $D2$ .

to leading order<sup>2</sup>.

Finally, we show in figure 10 our best result for the function  $\Delta^{B \rightarrow D}(w)$  that enters in the decay rate of the process  $B \rightarrow D\tau\nu_\tau$  (see discussion at the end of section II).  $\Delta^{B \rightarrow D}(w)$  does not show any significant dependence upon  $w$  and is very well approximated by its static limit (see eq. 6). These findings represent a prediction that can be confirmed by a future measurement of the differential decay rate of the process  $B \rightarrow D\tau\nu_\tau$ . Indeed, the function  $\Delta^{B \rightarrow D}(w)$  can be extracted experimentally by the ratio  $d\Gamma^{B \rightarrow D\tau\nu_\tau}/d\Gamma^{B \rightarrow D(e,\mu)\nu_{e,\mu}}$  that does not depend upon the CKM matrix element. On the other hand, the knowledge of  $\Delta^{B \rightarrow D}(w)$  is required in order to perform lepton-flavour universality checks on the extraction of  $V_{cb}$ .

## VII. CONCLUSIONS

We have performed the calculation of the form factors that parametrize semileptonic transitions among pseudoscalar heavy-light mesons and made a prediction for the ratio  $d\Gamma^{B \rightarrow D\tau\nu_\tau}/d\Gamma^{B \rightarrow D(e,\mu)\nu_{e,\mu}}$ . In view of a future measurement of the differential decay rate of the process  $B \rightarrow D\tau\nu_\tau$ , our results will allow to perform lepton-flavour universality checks on the extraction of  $V_{cb}$ .

The form factors have been obtained with a relative accuracy of the order of a few percent allowing to establish the range of validity of the heavy quark effective theory for these quantities. In particular we have obtained a check of the predictions of the Luke's theorem that we re-derived. The corrections to the static limit are very small already in the case of the elastic form factor  $h_+^{D \rightarrow D}$  and negligible in the case of  $h_+^{B \rightarrow B}$ . We have also established the accuracy of the static approximation to the form factors of the decay  $B \rightarrow D\ell\nu$  which is of the order of 2-3% at zero recoil and reaches about 7% at  $w = 1.2$  where becomes definitely inadequate for precise phenomenological applications.

Our results have been obtained within the quenched approximation and further calculations will be needed to assess the corrections due to unquenching. On the other hand, the accuracy reached in the quenched case demonstrates the feasibility and the opportunity of repeating the present calculation in the unquenched theory. Indeed, the recursive matching process can be extended to the sea quark masses that, alternatively, can be kept to their physical values if the Schrödinger Functional formalism is used. Moreover, flavour twisted boundary conditions can be used for heavy valence quarks also in the  $N_f = 3$  unquenched theory. The real case will further differ by the heavy flavour determinants that can be accounted for by a perturbative expansion in the hopping parameter.

<sup>2</sup> for a recent lattice calculation of the Isgur-Wise function see ref. [32]

### Acknowledgments

We warmly thank E. Molinaro for his participation at an early stage of this work. The simulations required to carry on this project have been performed on the INFN apeNEXT machines at Rome "La Sapienza". We thank A. Lonardo, D. Rossetti and P. Vicini for technical advice.

- 
- [1] N. Cabibbo, Phys. Rev. Lett. **10** (1963) 531.
  - [2] M. Kobayashi and T. Maskawa, Prog. Theor. Phys. **49** (1973) 652.
  - [3] N. Isgur and M. B. Wise, Phys. Lett. B **237** (1990) 527.
  - [4] B. Aubert *et al.* [BABAR Collaboration], arXiv:0707.2758 [hep-ex].
  - [5] A. Matyja *et al.* [Belle Collaboration], arXiv:0706.4429 [hep-ex].
  - [6] K. Kiers and A. Soni, Phys. Rev. D **56** (1997) 5786 [arXiv:hep-ph/9706337].
  - [7] C. H. Chen and C. Q. Geng, JHEP **0610** (2006) 053 [arXiv:hep-ph/0608166].
  - [8] G. M. de Divitiis, E. Molinaro, R. Petronzio and N. Tantalo, arXiv:0707.0582 [hep-lat].
  - [9] M. Guagnelli, F. Palombi, R. Petronzio and N. Tantalo, Phys. Lett. B **546** (2002) 237 [arXiv:hep-lat/0206023].
  - [10] G. M. de Divitiis, M. Guagnelli, F. Palombi, R. Petronzio and N. Tantalo, Nucl. Phys. B **672**, 372 (2003) [arXiv:hep-lat/0307005].
  - [11] G. M. de Divitiis, M. Guagnelli, R. Petronzio, N. Tantalo and F. Palombi, Nucl. Phys. B **675**, 309 (2003) [arXiv:hep-lat/0305018].
  - [12] D. Guazzini, R. Sommer and N. Tantalo, PoS **LAT2006** (2006) 084 [arXiv:hep-lat/0609065].
  - [13] G. M. de Divitiis, R. Petronzio and N. Tantalo, Phys. Lett. B **595**, 408 (2004) [arXiv:hep-lat/0405002].
  - [14] P. F. Bedaque, Phys. Lett. B **593** (2004) 82 [arXiv:nucl-th/0402051].
  - [15] C. T. Sachrajda and G. Villadoro, Phys. Lett. B **609**, 73 (2005) [arXiv:hep-lat/0411033].
  - [16] J. M. Flynn, A. Juttner and C. T. Sachrajda [UKQCD Collaboration], Phys. Lett. B **632**, 313 (2006) [arXiv:hep-lat/0506016].
  - [17] M. E. Luke, Phys. Lett. B **252** (1990) 447.
  - [18] A. F. Falk and M. Neubert, Phys. Rev. D **47** (1993) 2965 [arXiv:hep-ph/9209268].
  - [19] J. G. Korner and G. A. Schuler, Z. Phys. C **46** (1990) 93.
  - [20] M. Luscher, R. Narayanan, P. Weisz and U. Wolff, Nucl. Phys. B **384** (1992) 168 [arXiv:hep-lat/9207009].
  - [21] S. Sint, Nucl. Phys. B **421**, 135 (1994) [arXiv:hep-lat/9312079].
  - [22] M. Guagnelli, R. Sommer and H. Wittig [ALPHA collaboration], Nucl. Phys. B **535** (1998) 389 [arXiv:hep-lat/9806005].
  - [23] S. Necco and R. Sommer, Nucl. Phys. B **622**, 328 (2002) [arXiv:hep-lat/0108008].
  - [24] M. Guagnelli, R. Petronzio and N. Tantalo, Phys. Lett. B **548**, 58 (2002) [arXiv:hep-lat/0209112].
  - [25] M. Luscher, S. Sint, R. Sommer, P. Weisz and U. Wolff, Nucl. Phys. B **491** (1997) 323 [arXiv:hep-lat/9609035].
  - [26] S. Sint and P. Weisz, Nucl. Phys. B **502**, 251 (1997) [arXiv:hep-lat/9704001].
  - [27] G. M. de Divitiis and R. Petronzio, Phys. Lett. B **419** (1998) 311 [arXiv:hep-lat/9710071].
  - [28] S. Capitani, M. Luscher, R. Sommer and H. Wittig [ALPHA Collaboration], Nucl. Phys. B **544** (1999) 669 [arXiv:hep-lat/9810063].
  - [29] M. Guagnelli, R. Petronzio, J. Rolf, S. Sint, R. Sommer and U. Wolff [ALPHA Collaboration], Nucl. Phys. B **595**, 44 (2001) [arXiv:hep-lat/0009021].
  - [30] M. Neubert, Phys. Rev. D **46** (1992) 2212.
  - [31] M. Neubert, Phys. Rev. D **46** (1992) 3914.
  - [32] K. C. Bowler, G. Douglas, R. D. Kenway, G. N. Lacagnina and C. M. Maynard [UKQCD Collaboration], Nucl. Phys. B **637** (2002) 293 [arXiv:hep-lat/0202029].

	$\beta$	$T \times L^3$	$N_{cnfg}$	$k$	$\theta$
$L_0A$	7.300	$48 \times 24^3$	277	0.124176	0.000000
				0.124844	0.953456
				0.128440	1.201080
				0.129224	2.042983
				0.131950	2.573569
				0.134041	
$L_0B$	7.151	$40 \times 20^3$	224	0.122666	0.000000
				0.123437	0.953456
				0.127605	1.201079
				0.131511	1.719170
				0.131686	2.488490
				0.134277	
$L_0C$	6.963	$32 \times 16^3$	403	0.120081	0.000000
				0.120988	0.953456
				0.126050	1.201079
				0.131082	1.719170
				0.131314	2.488490
				0.134526	
	0.134614				
	0.134702				

TABLE II: Table of lattice simulations of the small volume.

$i \rightarrow f$	$w$	$G$	$h_+$	$h_-$
$D \rightarrow D$	1.00	1.000(00)	1.000(00)	
	1.03	0.979(02)	0.979(02)	
	1.05	0.967(03)	0.967(03)	
	1.10	0.942(04)	0.942(04)	
	1.20	0.894(06)	0.894(06)	
$B \rightarrow B$	1.00	1.000(00)	1.000(00)	
	1.03	0.980(02)	0.980(02)	
	1.05	0.969(03)	0.969(03)	
	1.10	0.940(05)	0.940(05)	
	1.20	0.882(09)	0.882(09)	
$B \rightarrow D$	1.00	1.025(17)	1.013(03)	-0.020(37)
	1.03	1.009(14)	0.992(03)	-0.032(29)
	1.05	1.000(13)	0.980(04)	-0.040(23)
	1.10	0.976(11)	0.953(04)	-0.048(17)
	1.20	0.929(09)	0.903(06)	-0.053(12)

TABLE III: Small volume results,  $L_0 = 0.4$  fm. Results corresponding to the definition  $D1$ .

	$\beta$	$T \times L^3$	$N_{cnfg}$	$k$	$\theta$
$L_{0a}$	6.737	$24 \times 12^3$	608	0.12490	0.000000
				0.12600	0.953456
				0.12770	1.201080
				0.12979	1.719172
				0.13015	2.488491
				0.13430	
				0.13460	
$L_{0b}$	6.420	$16 \times 8^3$	800	0.120674	0.000000
				0.122220	0.953456
				0.124410	1.201079
				0.127985	1.719172
				0.128066	2.488491
				0.134304	
				0.134770	
$L_{1A}$	6.737	$48 \times 24^3$	260	0.12490	0.000000
				0.12600	2.042983
				0.12770	2.573569
				0.12979	3.438340
				0.13015	4.976980
				0.13430	
				0.13460	
$L_{1B}$	6.420	$32 \times 16^3$	350	0.120674	0.000000
				0.122220	2.042983
				0.124410	2.573569
				0.127985	3.438340
				0.128066	4.976980
				0.134304	
				0.134770	
	0.135221				

TABLE IV: Table of lattice simulations of the first step.

$i \rightarrow f$	$w$	$\sigma_G$	$\sigma_+$	$\sigma_-$
$D \rightarrow D$	1.00	1.000(00)	1.000(00)	
	1.03	0.999(01)	0.999(01)	
	1.05	0.997(02)	0.997(02)	
	1.10	0.993(03)	0.993(03)	
	1.20	0.985(05)	0.985(05)	
$B \rightarrow B$	1.00	1.000(00)	1.000(00)	
	1.03	0.997(02)	0.997(02)	
	1.05	0.996(02)	0.996(02)	
	1.10	0.991(04)	0.991(04)	
	1.20	0.981(09)	0.981(09)	
$B \rightarrow D$	1.00	1.002(02)	1.003(01)	0.89(16)
	1.03	0.999(03)	1.000(02)	0.86(13)
	1.05	0.996(04)	0.998(02)	0.83(11)
	1.10	0.991(04)	0.993(03)	0.77(08)
	1.20	0.980(05)	0.983(05)	0.72(08)

TABLE V: First step, from  $L_0 = 0.4$  fm to  $L_1 = 0.8$  fm. Results corresponding to the definition  $D1$ .



	$\beta$	$T \times L^3$	$N_{cnfg}$	$k$	$\theta$
$L_{1a}$	6.420	$32 \times 16^3$	360	0.126600	0.000000
				0.127400	1.603930
				0.128030	2.080840
				0.128650	2.978423
				0.129500	4.311249
				0.134304	
				0.134770	
$L_{1b}$	5.960	$16 \times 8^3$	480	0.118128	0.000000
				0.119112	1.603930
				0.120112	2.080840
				0.121012	2.978423
				0.122513	4.311249
				0.131457	
				0.132335	
$L_{2A}$	6.420	$48 \times 24^3$	250	0.126600	0.000000
				0.127400	2.405895
				0.128030	3.121260
				0.128650	4.467634
				0.129500	6.200000
				0.134304	
				0.134770	
$L_{2B}$	5.960	$24 \times 12^3$	592	0.118128	0.000000
				0.119112	2.405895
				0.120112	3.121260
				0.121012	4.467634
				0.122513	6.200000
				0.131457	
				0.132335	
	0.133226				

TABLE VI: Table of lattice simulations of the second step.

$i \rightarrow f$	$w$	$\sigma_G$	$\sigma_+$	$\sigma_-$
$D \rightarrow D$	1.00	1.000(00)	1.000(00)	
	1.03	0.993(01)	0.993(01)	
	1.05	0.988(02)	0.988(02)	
	1.10	0.973(05)	0.973(05)	
	1.20	0.921(16)	0.921(16)	
$B \rightarrow B$	1.00	1.000(00)	1.000(00)	
	1.03	0.992(02)	0.992(02)	
	1.05	0.986(03)	0.986(03)	
	1.10	0.961(10)	0.961(10)	
	1.20	0.890(24)	0.890(24)	
$B \rightarrow D$	1.00	1.000(01)	1.000(01)	0.63(32)
	1.03	0.992(02)	0.993(02)	0.65(25)
	1.05	0.987(02)	0.988(02)	0.67(21)
	1.10	0.972(05)	0.972(05)	0.65(21)
	1.20	0.921(14)	0.921(14)	0.45(33)

TABLE VII: Second step, from  $L_1 = 0.8$  fm to  $L_2 = 1.2$  fm. Results corresponding to the definition  $D1$ .